Earth Planets Space, **57**, 961–972, 2005

Repeating short- and long-term slow slip events with deep tremor activity around the Bungo channel region, southwest Japan

Hitoshi Hirose and Kazushige Obara

National Research Institute for Earth Science and Disaster Prevention, 3-1 Tenno-dai, Tsukuba, Ibaraki, Japan

(Received August 31, 2004; Revised February 19, 2005; Accepted March 27, 2005)

We report the repeating occurrence of short- and long-term slow slip events (SSE) which are accompanied by deep tremor activity around the Bungo channel region, southwest Japan. Both of these activities are detected by NIED Hi-net, which is composed of densely distributed observatories equipped with a set of tiltmeter and a high-sensitivity seismograph. Since the short-term SSE is small in magnitude, GPS can detect only the long-term SSE. Some of these episodes have nearly the same surface deformation pattern. This shows the existence of 'slow slip patches' on a plate interface, where the episodic slow slip is the characteristic slip behavior. We observe a change in periodicity and size of the short-term episode after the onset of the long-term SSE. Moreover, the long-term slow slip accelerates when the short-term activity takes place. This suggests that there is an interaction between these two types of SSEs.

Key words: Subduction zone, Philippine Sea plate, plate interface, Hi-net, borehole tiltmeter, GPS, slow slip patch.

1. Introduction

At subduction zones, so called slow slip events (SSE) have been detected by geodetic measurements (e.g., Hirose, H. *et al.*, 1999; Hirose, I. *et al.*, 2000; Dragert *et al.*, 2001; Lowry *et al.*, 2001; Ozawa *et al.*, 2002, 2003). Most of these events have their own characteristic magnitude, duration, and recurrence rate, and they recur at almost the same location (Miller *et al.*, 2002; Kostoglodov *et al.*, 2003; Ozawa *et al.*, 2003, 2004). In this sense, like the concept of characteristic earthquake (e.g., Schwartz and Coppersmith, 1984), SSEs are also the characteristic mode of moment release at a deeper part of a subduction plate interface.

There is another characteristic phenomenon occurred at subduction zones. Obara (2002b) found a nonvolcanic deep low-frequency tremor activity along the Nankai trough subduction zone, southwest Japan. The tremor sources are distributed parallel to the strike of the subducted Philippine Sea slab. This suggests that the deep tremor activity relates to a dehydration process in the subducted slab (Obara, 2002b).

Recently, Rogers and Dragert (2003) reported that the occurrence of repeating SSE correlates with the nonvolcanic tremor activity in the Cascadia subduction zone. They call this phenomenon episodic tremor and slip. The similar phenomenon is detected in the southwest Japan subduction zone (Obara *et al.*, 2004). This information would be useful to constrain the generation mechanisms of both the tremor and the SSE.

Around the Bungo channel region, where the Philippine Sea plate subducts beneath the Amurian plate (Fig. 1), two types of SSEs are observed. One is a long-lasting SSE with about one-year duration (Hirose *et al.*, 1999; Ozawa *et al.*, 2004) and the other has short duration of nearly one week, a shorter recurrence interval, and coincides with deep tremor activity (Obara *et al.*, 2004). We call these two SSEs long-term SSE and short-term SSE, respectively. These source regions are adjacent to each other so that the long-term event might affect the generation of the short-term SSE, and vice versa.

In 2003, crustal deformation caused by these SSEs was observed in both tiltmeter and Global Positioning System (GPS) networks around the Bungo channel region. These events are accompanied by the deep tremor activity. In this article, we focus on the observational results of the crustal deformations due to the short- and long-term SSEs occurred in 2003 and early 2004. We demonstrate that both events are spatially and temporally close to each other. This may indicate that the occurrence of these events interacts with each other.

2. Data

2.1 Tiltmeters

National Research Institute for Earth Science and Disaster Prevention (NIED) operates a nationwide high-sensitivity seismograph network (Hi-net) with an average station interval of 20 km over Japan islands (Obara, 2002a; Okada *et al.*, 2004). Each Hi-net station has a sensor unit at the bottom of a borehole deeper than 100 m. Most Hi-net observatories are equipped with a high-sensitivity accelerometer in the sensor unit, whose long period horizontal component can be analyzed as ground tilt. Hereafter this instrument is referred to as tiltmeter.

We select six Hi-net stations in the western Shikoku region for analyzing the tiltmeter record (their locations are shown in Fig. 1). Generally, a tiltmeter is less stable for a

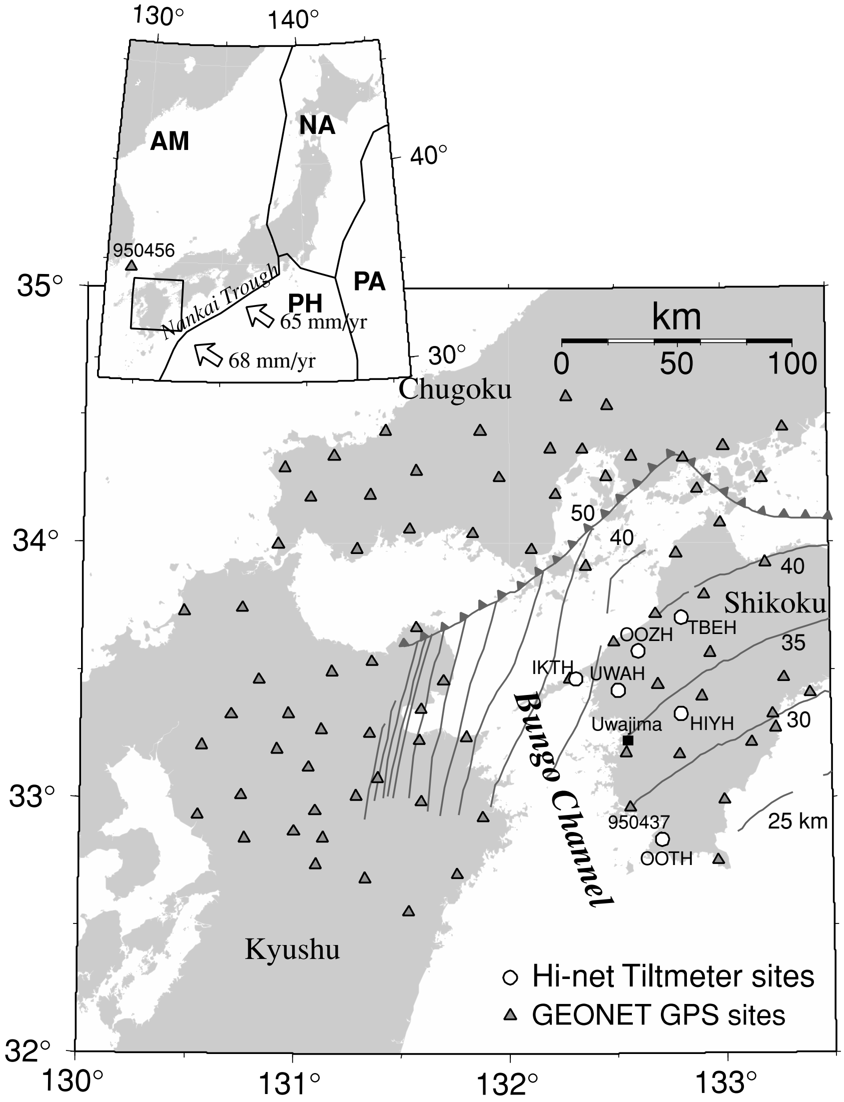

Fig. 1. Index map showing the study area. NA, AM, PA, and PH represent North American, Amurian, Pacific, and Philippine Sea plate, respectively. Open arrows denote the PH convergence rates with respect to AM (Miyazaki and Heki, 2001). Open circles and gray triangles show the Hi-net and the GEONET GPS station distribution, respectively. The location of Uwajima meteorological observatory is shown as solid square. The contour lines indicate the predominant focal depth of microearthquakes along the subducting Philippine Sea slab (Nakamura *et al.*, 1997).

long-term observation period than a short-term. For example, its record contains a long-term drift. We thus choose the tiltmeter records with enough stability to discuss crustal tilt changes for an interval of a few months.

The Hi-net tiltmeter signal is recorded with sampling frequency of 20 Hz. We resample this original 20 Hz record to one hour sampling data by averaging, and correct a sensor direction (Shiomi *et al.*, 2003). A borehole tiltmeter record often has steps caused by a strong seismic wave or other unidentified origins. We corrected them manually. We remove the tidal component and the response of atmospheric pressure estimated by BAYTAP-G (Tamura *et al.*, 1991). The atmospheric pressure record used in this procedure is observed at Uwajima meteorological observatory (Fig. 1). Additionally, a borehole tiltmeter time series record generally shows a long-term relaxation pattern, particularly just after the installation or the replacement of the sensor (e.g., Sato *et al.*, 1980). This pattern can be modeled as an exponential time function (e.g., NIED, 2002), so that we fit this function to the original data and then subtract this.

2.2 GPS

GPS daily coordinate data are processed and provided by Geographical Survey Institute of Japan (GSI). GSI operates nationwide GPS observation network named GEONET (Hatanaka *et al.*, 2003). In this study, we use 83 GPS stations in southwest Japan (Fig. 1). We choose the station 950456 (Kamitsushima) as a fixed station. We remove coordinate steps caused by large earthquakes, or maintenances at the site (e.g., an antenna setup change). We also remove a steady site velocity which represents a long-term tectonic motion and seasonal variations (Heki, 2001, 2004) by fitting a linear, an annual, and a biannual sinusoidal functions to each component of the station coordinate time series.

2.3 Tremors

Hourly tremor activity in southwest Japan is monitored by using Hi-net continuous data (Obara, 2002b). The tremor signals are characterized by long-lasting wave trains of low-frequency components between 1.5 and 10 Hz, lack

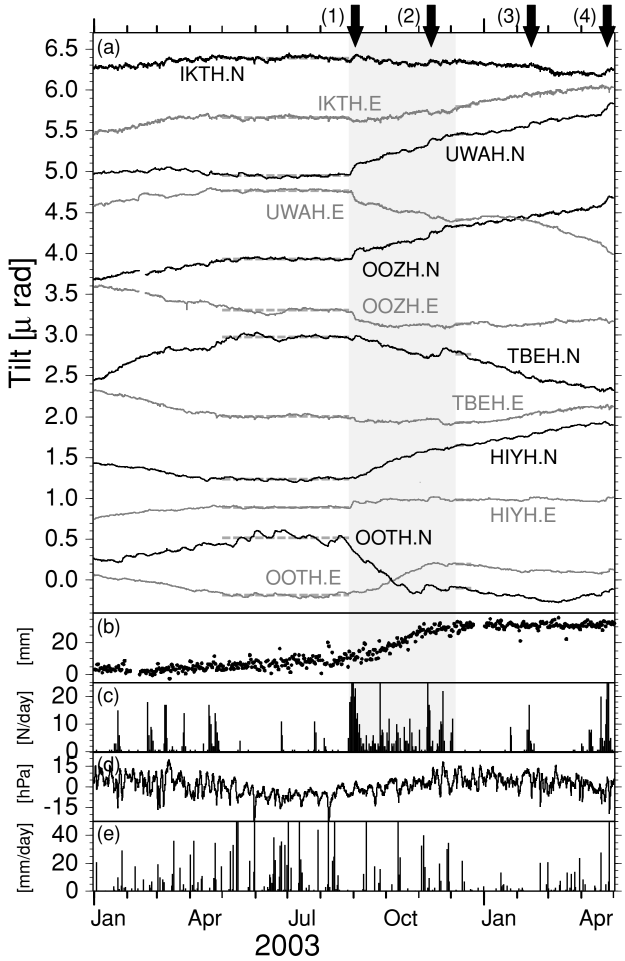

Fig. 2. Time series of observed crustal deformation, low-frequency tremor, and meteorological observations from January, 2003 to April, 2004. (a) Detrended tilt time series, (b) detrended GPS eastward displacement at 950437 (Misho, southwest Shikoku), (c) hourly count of tremor activity at west Shikoku, (d) atmospheric pressure and (e) daily precipitation at Uwajima meteorological observatory. The station locations are shown in Fig. 1. 'N' and 'E' followed by a station code with four characters in (a) denote the northward and eastward ground down components, respectively. Horizontal gray broken line segments before and after the episode show the fitted linear trends for the detrending. Gray shaded time window corresponds to an active period of 2003 Bungo Channel SSE. Solid arrows with a numeral represent the occurrence times of short-term slow slip events with tremor at the west Shikoku area. Note that the date and time in this article are in Japanese Standard Time (JST).

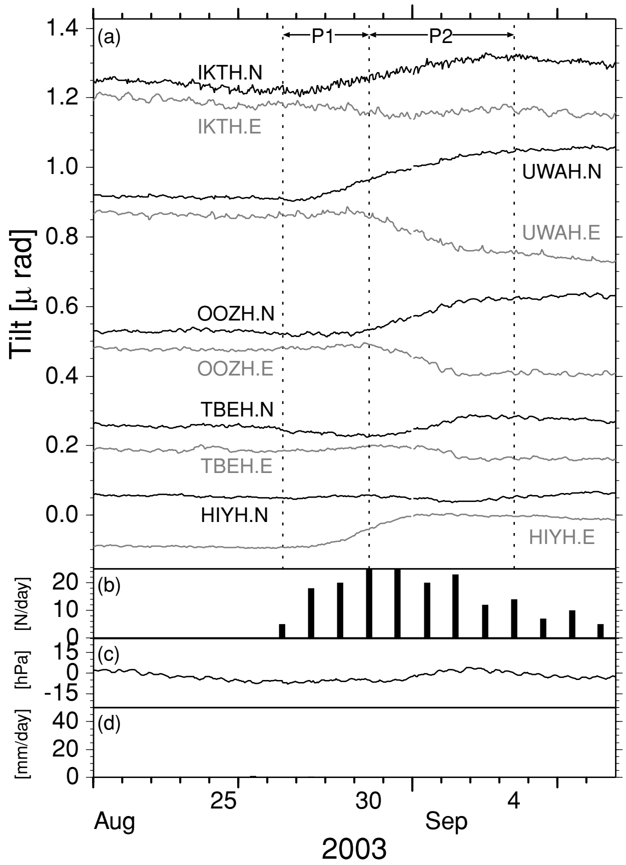

Fig. 3. Time series of observed tilt changes, low-frequency tremor, and meteorological observations from 21 August, 2003 to 7 September, 2003. (a) Detrended tilt time series. 'N' and 'E' followed by a station code with four characters denote the northward and eastward ground down components, respectively. (b) Hourly count of tremor activity at west Shikoku. (c) Atmospheric pressure and (d) daily precipitation at Uwajima meteorological observatory. 'P1' and 'P2' show the first and the second stages of the activity, respectively.

of distinct P or S phases, and gently-varying amplitude. The tremor sources are located by the envelope correlation method because of the lack of distinct P or S phases. See Obara (2002b) for detailed procedure of the tremor source determination.

3. Crustal Deformations and Tremor Activity at West Shikoku in 2003 and 2004

3.1 Overview of the activity

In general, the subduction tremors are extremely large scale phenomena characterized by a very wide source area over 600 km in length (Obara, 2002b). The continuation of the tremor monitoring reveals that the tremor sources are not distributed homogeneously in a narrow belt-like zone along the strike of the slab but some clusters exist in the zone (Obara *et al.*, 2004). Some of the clusters are activated quasi-periodically. One of these clusters is located in the western Shikoku region (Obara *et al.*, 2004).

In the west Shikoku region, we observe four episodes of simultaneous occurrence of the short-term SSE and the deep tremor, and their recurrence rate is about six months for two years from the beginning of 2001 (Obara *et al.*, 2004). From this quasi-periodicity, we expect that the next episode could happen in the early 2003. However, we cannot identify the short-term episode in this period, though some minor tremor activities are observed from January to April, 2003 (Fig. 2(c)).

The next obvious short-term episode arose in late August 2003 ('1' in Fig. 2). A step-like tilt change is observed at most of the stations. This episode contains the most active tremor since we started to monitor the tremor activity from 2001. Comparing a long-term trend of the tilt record before and after this short-term episode, we can determine that a change in the tilt trend emerges at these stations (Fig. 2(a)). The intermittent tremor activity which began late August 2003 lasts for almost three months (gray shaded period in Fig. 2). This is the first time that we continuously detect the tremor activity for such a long time period. The long-term

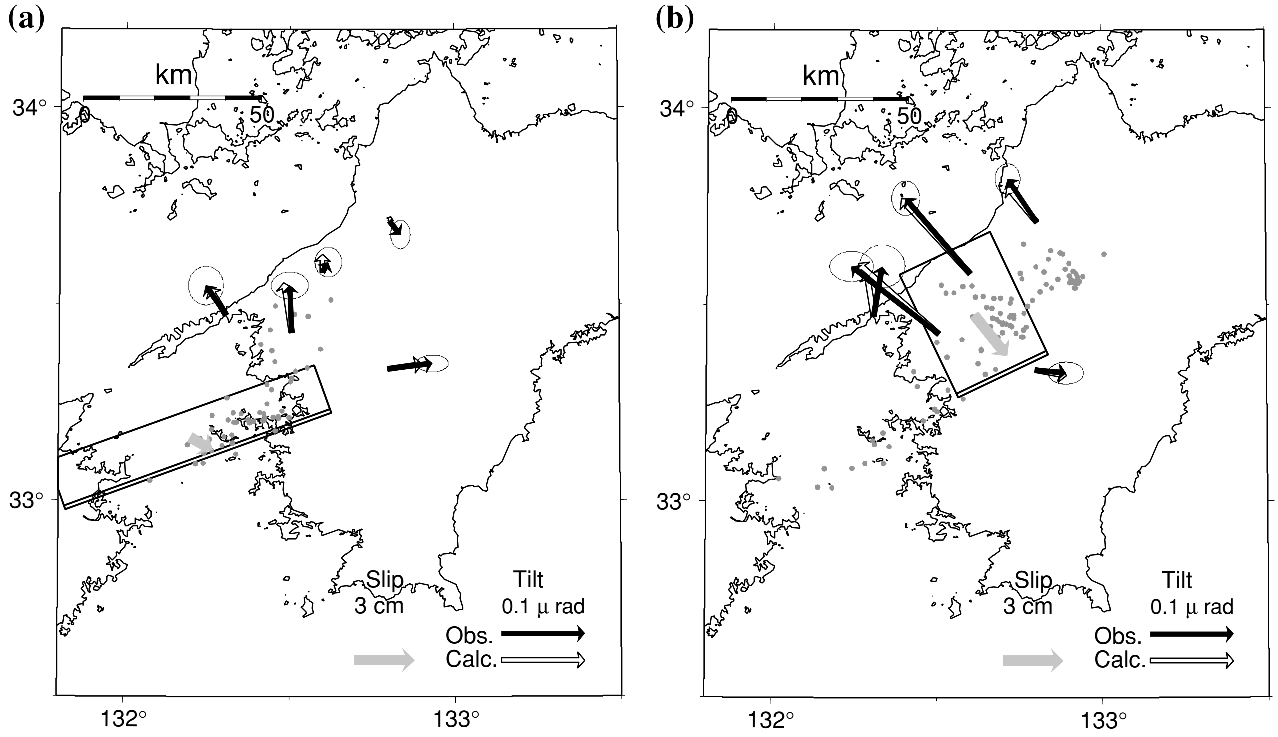

Fig. 4. The observed tilt changes (solid arrow), the estimated fault geometry (rectangles) and slip (thick gray arrows), and the calculated tilt changes (open arrows) for the successive two stages of the August 2003 short-term episode. Gray circles show the epicenter of the tremor identified in each time period. (a) The early stage (P1 in Fig. 3), and (b) the late stage (P2 in Fig. 3) of the episode. Error ellipses show 67% confidence limit.

Table 1. Estimated fault parameters and their errors for slow slip events in west Shikoku and Bungo Channel.

Event	Latitude (deg.)	Longitude (deg.)	Depth (km)	Length (km)	Width (km)	Strike (deg.)	Dip (deg.)	Slip (cm)	Rake (deg.)	M_0 10^{18} Nm	M_w
2003†	32.97	132.73	28.2	71	56	249	7	10.90	128	17.2	6.8
S. D.	0.19	0.18	8.1	19	18	17	11	0.56	26	7.3	–
Aug. 2003* P1	33.223	132.627	21.7	80	20.3	250.0	45.0	1.28	131	0.83	5.9
S. D.	0.043	0.059	5.3	14	6.4	3.9	6.2	0.43	22	0.41	–
Aug. 2003* P2	33.374	132.836	32.1	28	39.0	244.7	10.2	2.64	103.4	1.16	6.0
S. D.	0.034	0.025	3.3	12	5.1	3.2	3.8	0.24	4.9	0.53	–
Nov. 2003*	33.324	132.922	45.0	66	43.9	243.3	37.7	2.41	104.1	2.81	6.2
S. D.	0.053	0.025	1.9	12	5.6	2.4	3.8	0.35	7.1	0.75	–
Feb. 2004*	33.172	132.57	41.7	28	47.1	235.3	27.6	2.10	118	1.11	6.0
S. D.	0.070	0.16	3.1	13	6.6	3.9	4.6	0.52	14	0.60	–
Apr. 2004*	33.559	133.021	23.3	69	26.7	235.5	26.1	0.79	69	0.58	5.8
S. D.	0.059	0.065	6.2	16	8.9	7.1	7.8	0.16	11	0.26	–

†Long-term SSE; *Short-term SSE; M_0: Seismic moment (rigidity is assumed to be 40 GPa); M_w: Moment magnitude; *S. D.*: Standard deviation. *S. D.* is calculated among inverted parameters from bootstrap samples (pseudo-data) which are generated as the observed data plus a random noise.

tilt changes seemed to finish along with the termination of the long-term tremor activity. At the same time, a GPS site velocity began to change, and its anomalous movement lasts for the same period as the tilt changes and the tremor activity (Fig. 2(b)). The similar surface displacement time series is also detected at stations around the Bungo channel (Ozawa *et al.*, 2004). In 1997, the GEONET GPS sites recorded the similar signals, that is, the Bungo channel slow slip event (e.g., Hirose *et al.*, 1999). Accordingly, the same phenomenon reappears after approximately six year interval.

During the long-term episode, we detect another short-term episode (‘2’ in Fig. 2). The step-like tilt changes and the activation of the tremor similar to those appeared in August 2003 are observed in early November 2003. This episode is an unexpected one because only two months elapse since the previous episode, comparing with the average recurrence rate of about six months (Obara *et al.*, 2004).

In late November 2003, another short-term episode was observed in the central Shikoku area. The small tilt changes, especially in OOZH, and the accompanied tremor activity can be seen in Fig. 2, though the main activity is located in

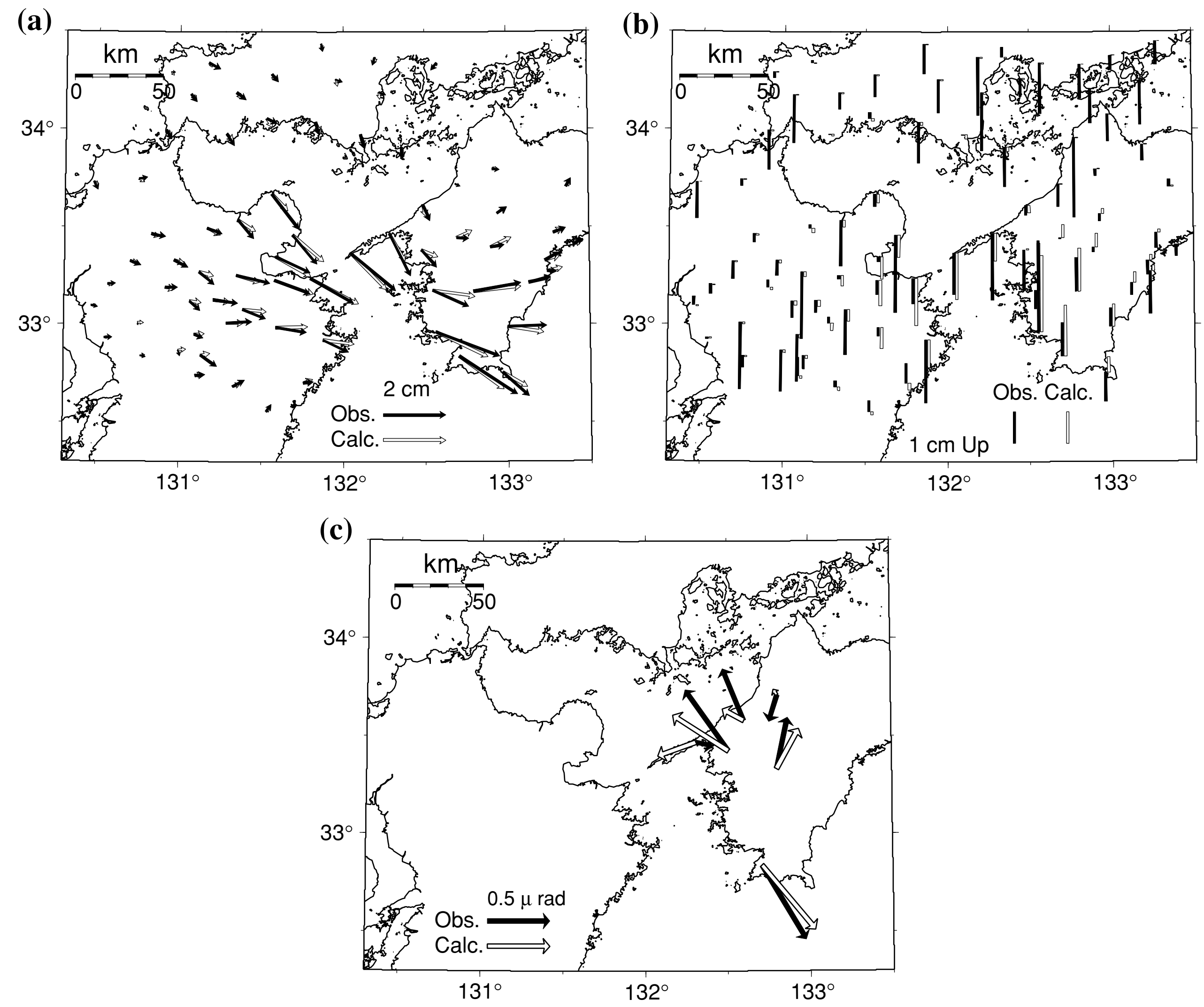

Fig. 5. Comparison between observed (solid symbols) and calculated (open symbols) crustal deformation due to the 2003 Bungo Channel slow slip event. The inverted fault model is shown in Fig. 6. (a) Horizontal displacements, (b) vertical displacements, and (c) tilt changes. The direction of the arrows in (c) corresponds to the ground down direction.

the east of the focused region. Because the source parameters for this slip episode cannot be inverted using the selected stations (Section 2.1), this episode is out of the scope of this article and we do not describe it.

The following two episodes are found in February and April, 2004 (‘3’ and ‘4’ in Fig. 2, respectively). The tilt changes during these episodes are slightly smaller than those in the previous ones. In addition, since August 2003 the recurrence rate of the short-term episodes decreases and is around three months, and the regularity is lost. This fact strongly suggests that the long-term SSE affects the generation and recurrence of the short-term SSEs.

In the following sections, we discuss the detailed observation results and the estimation of the slow slip fault models from the geodetic data for each episode.

3.2 August 2003 short-term slow slip event with tremor

Figure 3 shows a close-up view of the time series of the short-term episode started in late August 2003. The coherent slow tilt signals and the correlated tremor activity which last for a week are clearly observed, and they do not correspond to the changes in atmospheric pressure or precipitation. In addition, the emergence of the tremor activity precedes the starting of the tilt changes. The ground tilt at IKTH and UWAH, which are located in the western part of the focused area (Fig. 1), began to change on August 28. The change in HIYH followed within a day. That in OOZH and TBEH appeared with nearly two days delay. This evidence suggests that the source area migrates from west to east. The maximum tilt change is 0.19 μrad recorded at UWAH. These observed features are similar to the ‘summer type activity’ (Obara *et al.*, 2004) found in August 2001 and 2002, except for little change in the NS component in HIYH.

The tilt change in UWAH shows an attractive feature. The northward tilt precedes the start of the westward tilt almost two days. This means that UWAH began to tilt in the northward direction at the beginning, and then changed the direction to the northwest. This change in tilt direction indicates that an uplift region migrates from the south of UWAH to the southeast and suggests the migration of the slow slip source to the same direction.

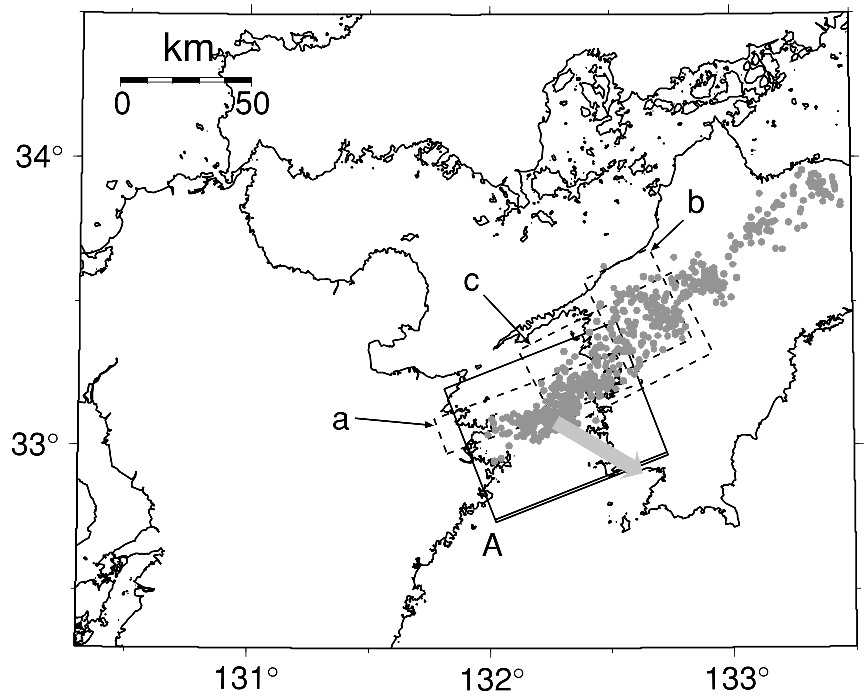

Fig. 6. An estimated fault model for the 2003 Bungo Channel slow slip event (fault 'A'). A gray arrow denotes a slip vector on the fault. Dotted rectangles show fault locations of short-term SSEs with tremor occurred during the active period of 2003 long-term Bungo Channel SSE: (a) the early stage of the August 2003 event, (b) the late stage of the August 2003 event, and (c) November 2003 event. Gray dots represent the epicenters of tremor activity occurred during the long-term SSE (gray shaded time interval in Fig. 2).

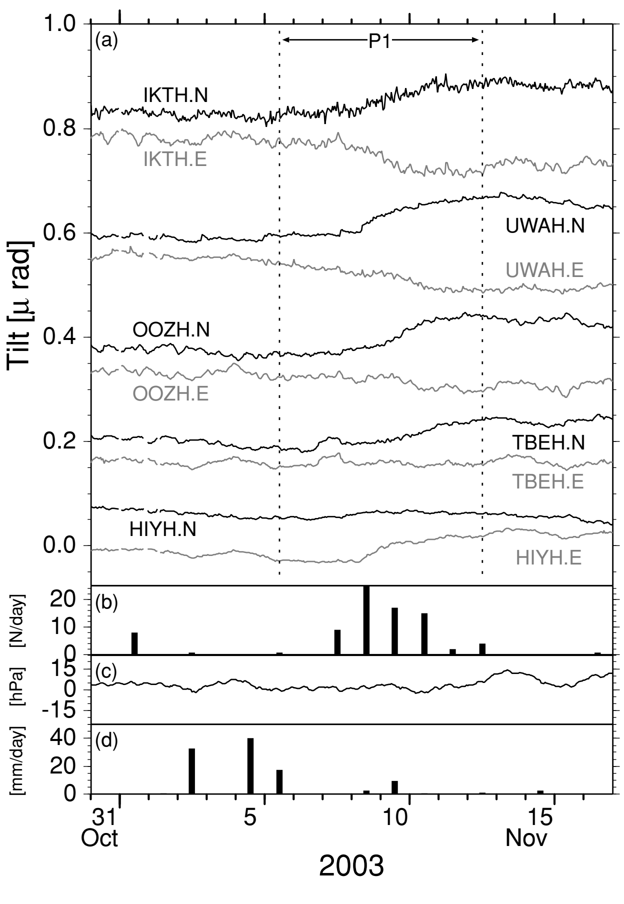

Fig. 7. Same as Fig. 3 but for the time period from 31 October to 17 November, 2003. The time window labeled 'P1' shows the identified interval of SSE with tremor.

In order to clarify the migration of the source, we divide this episode into two time periods, the early and the late stages (P1 and P2 in Fig. 3). In each stage, we measure a tilt change vector for each station by comparing the averages in two one-day time windows, one is the earliest window and the other is the latest in a stage. A confidence limit σ for each tilt vector is assumed to be a superposition of a random walk noise ($\sigma_{\rm rw}$) and a white noise ($\sigma_{\rm w}$) components (e.g., Langbein and Johnson, 1997), i.e., $\sigma^2 = \sigma_{\rm w}^2 + \sigma_{\rm rw}^2\, T$, where T is a length of time interval. Typical values of $\sigma_{\rm w}$ and $\sigma_{\rm rw}$ for the tiltmeter records are 1×10^{-2} μrad and 3×10^{-3} μrad $/\sqrt{\rm day}$, respectively. Note that we exclude the tilt record of the station OOTH, around 50 km south of the tremor sources in west Shikoku, from the analysis of the short-term episodes because of its insufficient signal amplitude. We then use the remaining five stations as homogeneous stations to discuss relative locations of the short-term slow slip sources.

The resultant tilt change vectors are plotted in Fig. 4 (solid arrows). As noticed above, we can see the changes in tilt direction, especially at UWAH and OOZH, for two successive stages. Based on these tilt change data, we then estimate the slow slip fault parameters for each stage. We assume a simple rectangular fault in an elastic half-space. A rectangular fault can be defined by nine parameters. To estimate these parameters from the tilt change data, we apply the genetic algorithm to non-linear parameters, such as the position, the dimensions, and the direction of the fault, and the weighted least squares method to linear parameters, i.e., the slip vector on the fault. In the inversion procedure, Okada's (1992) analytical expression is adopted.

The estimated fault models are plotted in Fig. 4 with

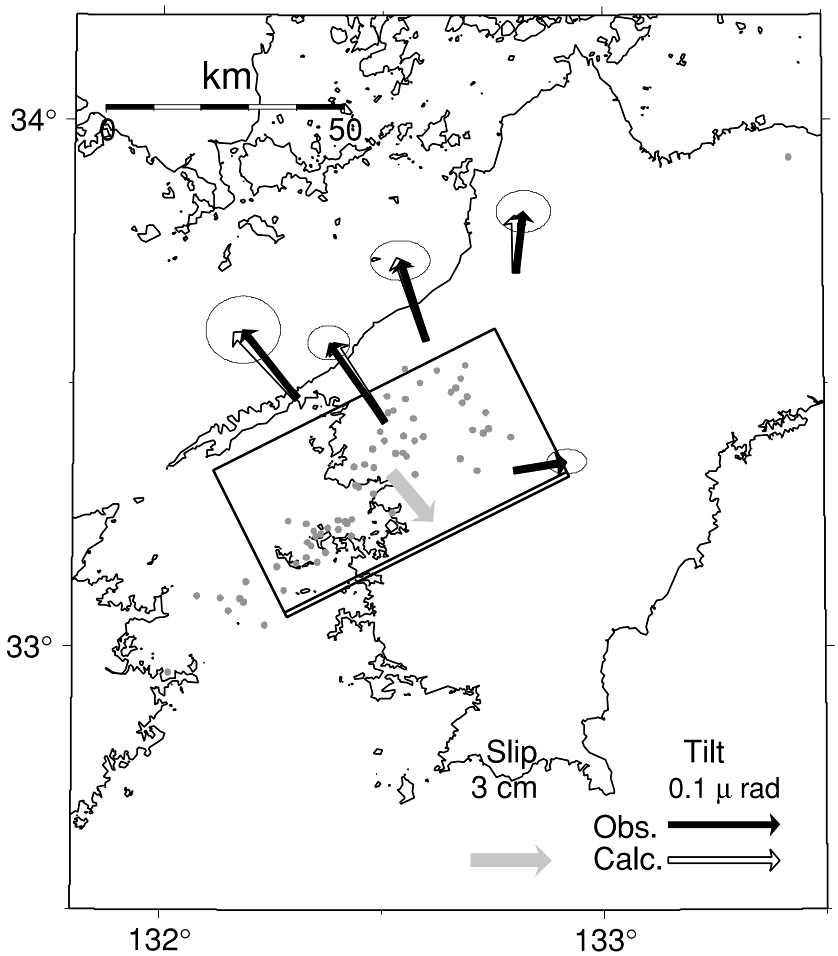

Fig. 8. Same as Fig. 4 but for the episode in late November 2003 (Fig. 7).

the locations of the tremors identified in each stage, and the fault parameters are listed in Table 1. The low-angle thrust faults with slip direction which is opposite to the convergent direction of the subducting Philippine Sea plate with respect to the hanging wall side, Amurian plate are retrieved. The depth of the faults roughly corresponds to that of the plate interface. In the early stage (P1), the main part of the slow slip fault is located in the western part, beneath the Bungo channel region. Most of the tremors are also located there. In the late stage (P2), in turn, the slip area and the location of the tremors migrate to the northeast direction. This source migration direction is the same as the 'summer type' (Obara *et al.*, 2004). Comparing the slip area with that of the episode in August 2002, however, the northeasternmost part of the slip area in August 2002 does not slip in August 2003. This is supported by the fact that the lack of tilt change in the NS component in HIYH. The released seismic moment during this slow slip sequence corresponds to a moment magnitude (M_w) 6.1, which is slightly larger than the average (M_w 6.0) for the four episodes observed in 2001 and 2002 (Obara *et al.*, 2004). This may be related to the absence of clear evidence of the short-term activity in the early 2003. Note that the calculated tilt vectors show that the observed tilt changes are almost reproduced by the estimated models (Fig. 4).

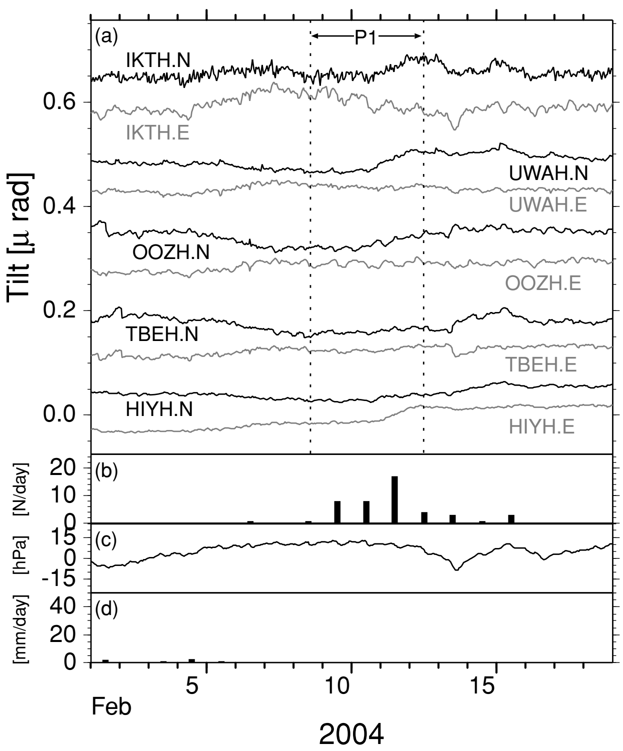

Fig. 9. Same as Fig. 3 but for the time period from 2 to 19 February, 2004.

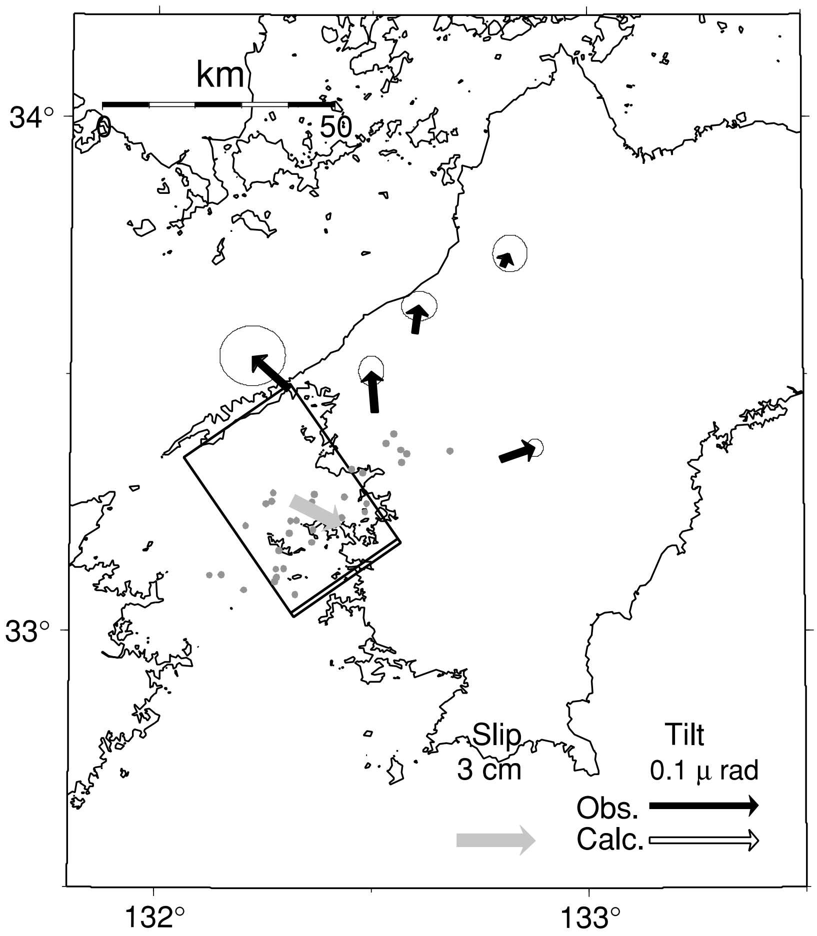

Fig. 10. Same as Fig. 4 but for the episode in February 2004 (Fig. 9).

3.3 2003 long-term slow slip event

As we already mentioned, the anomalous long-term crustal tilt changes and the intermittent tremor activity started in late August 2003 (Fig. 2(a) and (c)). At the same time, the surface displacement accelerated (Fig. 2(b)). However, a small gradual change in displacement time series seems to appear in early 2003 (Fig. 2(b)). Although the absolute displacement is not greater than a significant level and there may be an effect of the antenna changes (Ozawa *et al.*, 2004) in some degrees, the displacement time function is very similar to that in the previous 1997 SSE, including the very small and gradual displacement change in the beginning and the relatively accelerated phase lasted for roughly three months near the end of the event (e.g., Hirose *et al.*, 1999).

We calculate tilt changes and GPS horizontal and vertical displacements between August and December 2003 as crustal deformation due to the long-term SSE. Solid arrows and bars in Fig. 5 denote these observed displacements and tilt changes. Surprisingly, the spatial pattern of the horizontal displacement vectors (Fig. 5(a)) appears to be approximately the same as that in the previous SSE (e.g., Hirose *et al.*, 1999). This suggests that the same phenomenon, the long-term SSE, occurs again, and furthermore, both the two events share nearly the same source area.

Using those tilt change and the GPS horizontal and vertical displacement data, we estimate the fault parameters for the 2003 long-term SSE by the same way as described in the previous section. The estimated fault location and the slip vector are shown in Fig. 6 and the estimated parameters are noted in Table 1. Again, a shallow dipping reverse fault with southeastward slip direction is estimated. The inverted slip area ranges between Shikoku and Kyushu, beneath the Bungo channel. The slip area partly overlaps that of the early stage of the August 2003 short-term SSE and extends to a shallower part, although the confidence limit of the fault position and the area is relatively large.

Figure 6 also shows the tremor epicenters which occurred during the active period of the long-term SSE. Most of the tremors are located in the estimated fault region of the long-term SSE (‘A’ in Fig. 6). The tremors located outside of this region are mostly accompanied by the two short-term SSEs occurred in November 2003. In other words, the intermittent but active long-term tremors during this period (Fig. 2(c)) are correlated with the long-term SSE.

In Fig. 5, the calculated surface displacements and tilt changes due to the estimated fault slip are plotted as well as the observed ones. The calculated tilt changes in addition to the calculated surface displacements match well with the observed ones. This indicates that not only the detailed source model (Ozawa *et al.*, 2004) but also this simple rectangular fault model can explain the observed crustal deformation data.

3.4 Short-term episodes following the 2003 long-term event

Near the end of the long-term episode discussed above, we observe another short-term episode in early November 2003. Figure 7 shows a detailed time series. Although some disturbances in the tilt records probably due to rainfall are found around October 5, clear coherent slow tilt buildups and the tremor activity appear simultaneously from October 8 to 12. A slow slip fault is inverted from the tilt changes for seven-day time period ('P1' in Fig. 7). The fault area ranges between the Bungo channel and the western part of Shikoku (Fig. 8 and 'c' in Fig. 6). This covers the slip area for the second stage in August 2003 episode ('b' in Fig. 6), whereas this does not contain most of the area for the first stage ('a' in Fig. 6).

The next short-term episode in west Shikoku happens in February 2004. In this episode, the recorded tilt change is smaller than that in the past episodes (Fig. 9). Among them, the tilt change is relatively larger at the site near the Bungo channel (solid arrows in Fig. 10). This indicates that the slip area is limited within the western part, the Bungo channel region (Fig. 10). In addition, the duration of this episode is 3–4 days, which is relatively shorter than that of the earlier episodes (Fig. 9). Also, the observed tilt vectors and the estimated fault location (Fig. 10) are similar to those in the early stage of the August 2003 episode (Fig. 4(a)). These features suggest that only the source region of the early stage of the August episode is activated and that of the late stage remains unslipped in the February 2004 episode.

Two months later since the February episode, another short-term episode is detected (Fig. 11). Because heavy rain on April 19 and 27 affects the tilt record of some stations, we assume the episode lasts for five days from 22 to 27. The active tremor begins on 19, so that some changes due to the SSE might be contained in the tilt records. Therefore this assumption may lead to underestimation of the magnitude and the duration of the event. The spatial pattern of the tilt changes (solid arrows in Fig. 12) is similar to that in November 2003 (Fig. 8) except for the NS tilt component at HIYH. In the November 2003 episode, HIYH shows little change in ground tilt in southward down direction (Figs. 7 and 8) and almost eastward down tilt, whereas in the April 2004 episode, southeastward down tilt at HIYH is observed (Fig. 12). This would reflect the difference in the northeastward extension of the slip region of both two episodes. That is, the northeastern end of the estimated fault and the tremor epicenters in the April 2004 episode (Fig. 12) are located in about 20 km to the northeast from the northeastern end of those in the November 2003 episode (Fig. 8).

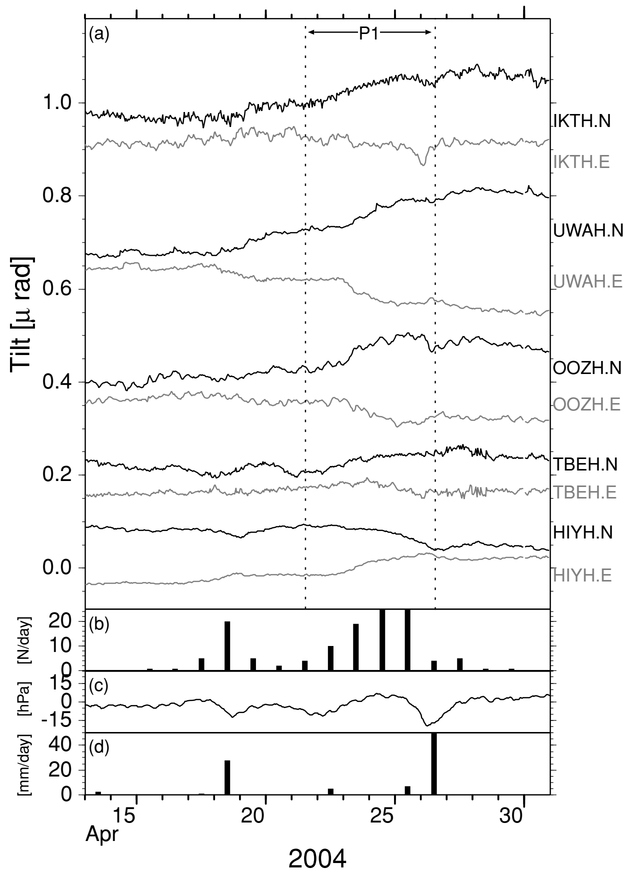

Fig. 11. Same as Fig. 3 but for the time period from 14 April to 1 May, 2004.

4. Discussion

We observed the repeating slow slip events with the deep tremor activity around the Bungo channel region in southwest Japan by NIED Hi-net. This is the same phenomenon as that detected in the Cascadia subduction zone (Rogers and Dragert, 2003). The subduction tremor is thought to be a manifestation of dehydration process in the subducted slab (Obara, 2002b). If the liberated fluid is injected into the plate interface, then pore fluid pressure increases and an effective normal stress decreases. This leads to a slip under lower stress conditions. Under the lower stress, a slip velocity is expected to be slower (e.g., Brune, 1970), and a SSE is likely to occur. In this scenario, the fluid plays a very important role in generating both tremors and SSEs.

The relative locations of the slow slip faults with respect to the tremors are important information to constrain the generation mechanism for this coupling phenomenon. Our solutions imply that most of the tremor sources are distributed in the coincident short-term slow slip areas (Figs. 4, 8, 10, and 12), whereas the tremor locations correspond to the deeper part of the long-term slow slip fault (Fig. 6). From the other point of view, a centroid of a moment release of the long-term SSE is located on the forearc side of the tremor belt, i.e., the shallower part on the plate interface than that of the short-term SSE.

These results would give rise to the following two important issues which we should take into account. First, the relative location of the short- and long-term SSEs may imply the difference in the generation mechanism of these two SSEs. Second, the location of the SSE relative to the tremor may reflect the difference in the interaction between the short- or long-term SSE and the accompanied tremor.

The first issue indicates the transition in slip behaviors along dip of the subduction plate boundary. That is, the short-term SSE, which has several days' duration, repeats at intervals of 2–6 months on the deeper portion of the boundary, the long-term SSE, which lasts for a year, recurs ev-

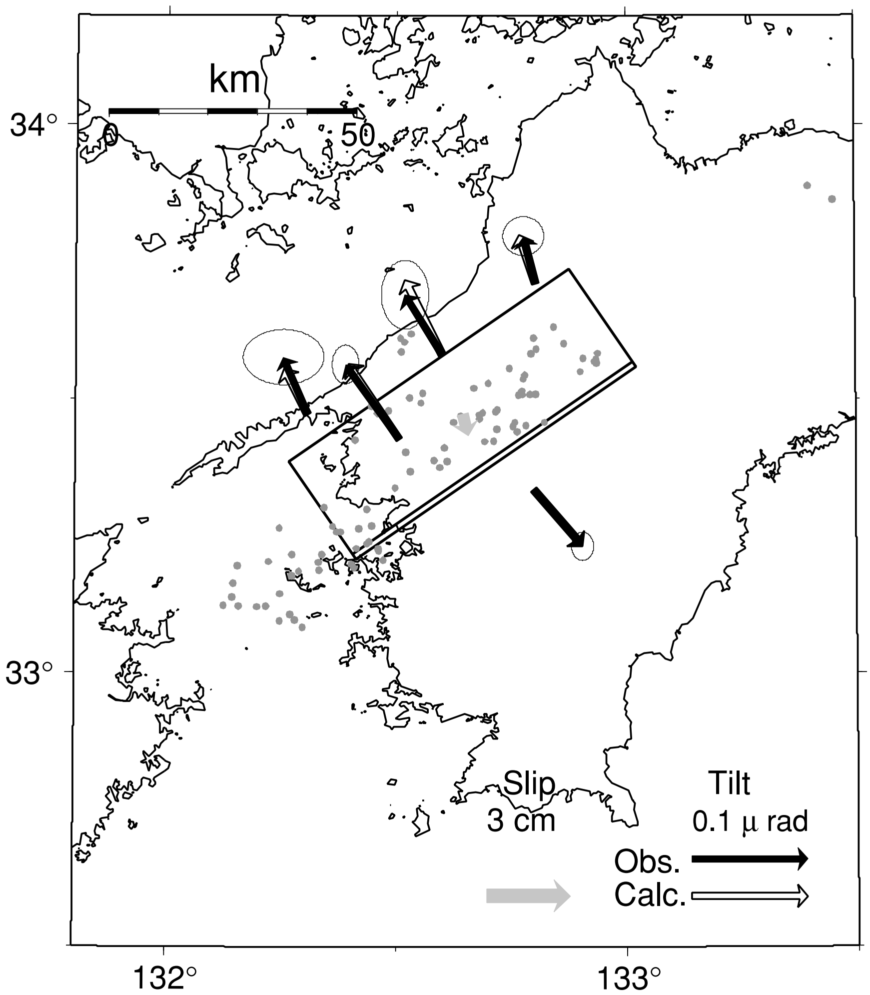

Fig. 12. Same as Fig. 4 but for the episode in April 2004 (Fig. 11).

ery six years on the shallower part, and on the shallowest part, the megathrust earthquakes repeatedly occur with an average recurrence interval of about a hundred years (e.g., Ando, 1975). This transition in slip behavior from a stable slip at the deeper part to unstable at the shallower portion can be reproduced by a simple spring-slider model with varying spring stiffness (e.g., Baumberger *et al.*, 1999). In this model, we observe the following features as slip stability changing from unstable to stable: (1) shortening of the recurrence interval; (2) consequent reduction in stress drop per one slip event, which is roughly proportional to the amount of slip in case with comparable fault dimensions; and (3) reduction in slip rate. In turn, the detected transition in slip behavior around the Bungo channel region could be roughly explained by this model for the above features (1) and (2), but for (3) because the shallower long-term SSE is likely to have a slower slip rate ($\sim$10 cm/year) than the deeper short-term SSE ($\sim$1 cm/day). This consideration also suggests the necessity of other mechanisms, possibly introducing the effect of the fluid, for explaining the occurrence of the short-term SSE at the deeper part.

The second issue would reflect that there are different relationships between SSE and tremor in these two kinds of SSEs with tremor, i.e., the generation mechanism of the short-term SSE and the correlating tremor may be different from that which act on the long-term SSE with tremor. A possible difference in the correlation mechanism is a way of connection between the SSE and the tremor activity. In the short-term activity, the liberated fluid may link them as mentioned above. In the long-term activity, on the other hand, SSE and the tremor might be two distinguishable phenomena and the tremor could be triggered by a stress perturbation due to the nearby long-term SSE. As Obara (2002b, 2003) suggested, the tremor activity would be sometimes triggered by a nearby earthquake or a teleseismic wave. This indicates that the tremor source region is very sensitive to various disturbances. In this situation, the relation between the long-term SSE and the tremor could be characterized by the triggering.

The short-term SSE with tremor in the west Shikoku region recurs with an interval of nearly six months for two years from 2001 (Obara *et al.*, 2004). During and after the 2003 long-term SSE, however, the recurrence rate decreases to roughly three months as we mentioned in the previous section. Furthermore, the activated source area during an episode is reduced, comparing it with that in 2001 and 2002 episodes. This suggests that a large moment release by the long-term SSE triggers the nearby short-term SSEs and hastens these occurrences. On the other hand, the timing of the acceleration of the long-term SSE in late August 2003

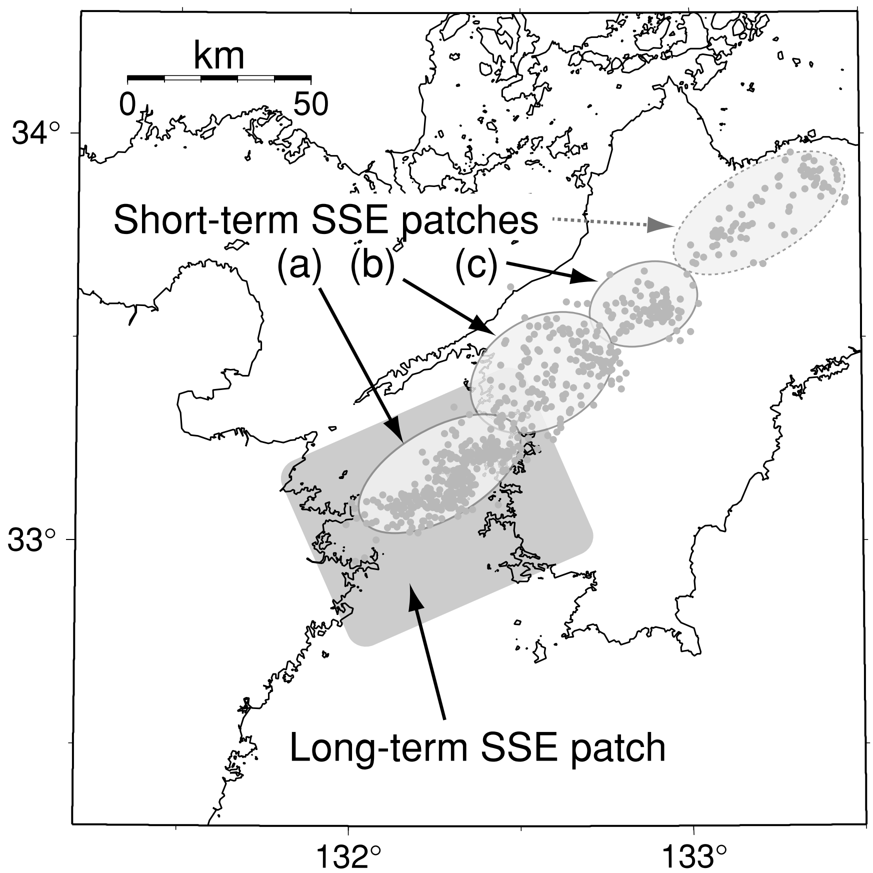

Fig. 13. Speculated distribution of slow slip patches. Gray ellipsoids denote the short-term SSE patches whereas gray round corner rectangle area represents the long-term SSE patch. Gray dots show the epicenters of the tremors.

completely coincides with the occurrence of the short-term episode. This implies that the short-term SSE works as a precursory slip which leads to a main phase of the long-term SSE. Therefore, there must be the interaction between the short- and the long-term SSEs.

These smaller episodes reveal the existence of the internal structure inside the slow slipping area, named 'slow slip patches.' The slow slip patch has its own characteristic size, strength, and slip behavior including the duration and the slip rate, and is distributed on a plate interface. These properties are almost constant during several recurrence cycles. This concept is an analogy of the 'asperity model' (Lay and Kanamori, 1981), which has recently been supported by observational studies (e.g., Nadeau and McEvilly, 1999; Nagai *et al.*, 2001; Yamanaka and Kikuchi, 2004).

Figure 13 shows a speculated distribution of slow slip patches on the plate interface. Below around 30 km depth, the plate interface is thought to be in a steady sliding state or a transitional state from a fully locked to the steady sliding state (Hyndman *et al.*, 1995). However, as we mentioned above, the observational results suggest that there are some particular regions where the slow slip events repeatedly occur at such a depth on the plate interface. This means that at these regions the interface is almost locked in a steady state and sometimes slips aseismically. Therefore we propose that there are the slow slip patches bordering the steady sliding regions and the locked regions. From our results, there may be at least three short-term SSE patches in the study area ('a', 'b', and 'c' in Fig. 13). That is, in the 2001 and 2002 episodes all three patches were activated sequentially. On the other hand, in August 2003 short-term episode the patches 'a' and 'b' slipped. Also 'b' in November 2003, 'a' in February 2004, and 'b' and 'c' in April 2004 were activated, respectively. Moreover, the observations imply that the slow slip patches around the Bungo channel region can be classified into at least two groups: One is the short-term SSE patches and the other is the long-term SSE patch. Our results indicate that the source area of the 2003 long-term SSE partly overlaps that of the August 2003 short-term SSE (Fig. 6). This may imply that some of the smaller short-term SSE patches are surrounded by the larger long-term SSE patch region, and these two regions are spatially separated.

The concept of slow slip patches is supported by the observed similarity in surface deformation patterns. As we pointed out in Section 3.4, the observed down tilt vector fields for the early stage of the August 2003 episode and the February 2004 episode are very similar to each other in magnitude and direction of the tilt changes. The same similarity is seen in a combination of those for November 2003 and April 2004 episodes. Moreover, the surface displacement fields for the 1997 and 2003 long-term SSE are also nearly the same (see figure 4 in Hirose *et al.*, 1999 and Fig. 5). This should be considered as the repeating slow slip events with characteristic size and a frictional property.

5. Conclusion

We detected the repeating activity of slow slip events with deep tremors around the Bungo channel region, southwest Japan by tiltmeters and short-period seismographs of NIED Hi-net and GPS of GEONET. There are two types of activity in this region, one is a short-term slow slip event with perfectly correlated tremors, and the other is a long-term slow slip event with intermittent tremors. Both of these activities would be the characteristic slip behaviors in each source area on a plate interface. These source regions should be called 'slow slip patches.' The short-term episode has a periodicity of about six months before the long-term episode in 2003, while such a regularity is lost after the long-term episode. In addition, the long-term slow slip accelerates when the short-term activity takes place. This suggests that there is an interaction between these two types of slow slip events.

Acknowledgments. We are grateful to K. Kasahara and F. Yamamizu for their valuable effort to develop and maintain the Hi-net observation network. We would like to thank Y. Tamura for providing the BAYTAP-G software. GPS coordinate time series data were provided by Geographical Survey Institute of Japan. Meteorological data were provided by Japan Meteorological Agency. Comments from S. Miyazaki and A. R. Lowry significantly improved the manuscript.

References

Ando, M., Source mechanisms and tectonic significance of historical earthquakes along the Nankai trough, Japan, *Tectonophys.*, **27**, 119–140, 1975.

Baumberger, T., P. Berthoud, and C. Caroli, Physical analysis of the state- and rate-dependent friction law. II. Dynamic friction, *Phys. Rev. B*, **60**, 3928–3939, 1999.

Brune, J. N., Tectonic stress and the spectra of seismic shear waves from earthquakes, *J. Geophys. Res.*, **75**, 4997–5009, 1970.

Dragert, H., K. Wang, and T. S. James, A silent slip event on the deeper Cascadia subduction interface, *Science*, **292**, 1525–1528, 2001.

Hatanaka, Y., T. Iizuka, M. Sawada, A. Yamagiwa, Y. Kikuta, J. M. Johnson, and C. Rocken, Improvement of the analysis strategy of GEONET, *Bull. Geogr. Surv. Inst.*, **49**, 11–37, 2003.

Heki, K., Seasonal modulation of interseismic strain buildup in Northeastern Japan driven by snow loads, *Science*, **293**, 89–92, 2001.

Heki, K., Dense GPS array as a new sensor of seasonal changes of surface loads, in *The State of the Planet: Frontiers and Challenges in Geophysics*, edited by R. S. J. Sparks and C. J. Hawkesworth, American Geophysical Union, Washington D. C., 2004.

Hirose, H., K. Hirahara, F. Kimata, N. Fujii, and S. Miyazaki, A slow thrust slip event following the two 1996 Hyuganada earthquakes beneath the Bungo Channel, southwest Japan, *Geophys. Res. Lett.*, **26**(21), 3237–3240, 1999.

Hirose, I., I. Kawasaki, Y. Okada, T. Sagiya, and Y. Tamura, A silent earthquake of December 9, 1989, in the Tokyo Bay, as revealed by the continuous observation of crustal movements in the southern Kanto district, central Japan, *Zisin, 2nd ser., J. Seism. Soc. Jpn*, **53**, 11–23, 2000 (in Japanese with English abstract).

Hyndman, R. D., K. Wang, and M. Yamano, Thermal constraints on the seismogenic portion of the southwestern Japan subduction thrust, *J. Geophys. Res.*, **100**(B8), 15,373–15,392, 1995.

Kostoglodov, V., S. K. Singh, J. A. Santiago, S. I. Franco, K. M. Larson, A. R. Lowry, and R. Bilham, A large silent earthquake in the Guerrero seismic gap, Mexico, *Geophys. Res. Lett.*, **30**(15), doi:10.1029/2003GL017219, 2003.

Langbein, J. and H. Johnson, Correlated errors in geodetic time series: Implications for time-dependent deformation, *J. Geophys. Res.*, **102**, 591–603, 1997.

Lay, T. and H. Kanamori, An asperity model of large earthquake sequences, in *Earthquake Prediction*, edited by D. W. Simpson and P. G. Richards, 680 pp., American Geophysical Union, Washington D. C., 1981.

Lowry, A. R., K. M. Larson, V. Kostoglodov, and R. Bilham, Transient fault slip in Guerrero, southern Mexico, *Geophys. Res. Lett.*, **28**(19), 3753–3756, 2001.

Miller, M. M., T. Melbourne, D. J. Johnson, and W. Q. Sumner, Periodic slow earthquakes from the Cascadia subduction zone, *Science*, **295**, 2423, 2002.

Miyazaki, S. and K. Heki, Crustal velocity field of southwest Japan: Subduction and arc-arc collision, *J. Geophys. Res.*, **106**(B3), 4305–4326, 2001.

Nadeau, R. M. and T. V. McEvilly, Fault slip rates at depth from recurrence intervals of repeating microearthquakes, *Science*, **285**, 718–721, 1999.

Nagai, R., M. Kikuchi, and Y. Yamanaka, Comparative study on the source processes of recurrent large earthquakes in Sanriku-oki region: the 1968 Tokachi-oki earthquake and the 1994 Sanriku-oki earthquake, *Zisin, 2nd ser., J. Seism. Soc. Jpn*, **54**, 267–280, 2001 (in Japanese with English abstract).

Nakamura, M., H. Watanabe, T. Konomi, S. Kimura, and K. Miura, Characteristic activities of subcrustal earthquakes along the outer zone of southwestern Japan, *Annu. Disaster Prev. Res. Inst. Kyoto Univ.*, **40**(B1), 1–20, 1997 (in Japanese with English abstract).

National Research Institute for Earth Science and Disaster Prevention (NIED), Viscosities of crustal rocks estimated from long-term continuous observation by Sakata-type three-component borehole strainmeters, *Rep. Coord. Commit. Eq. Pred.*, **67**, 138–146, 2002 (in Japanese).

Obara, K., Hi-net: High sensitivity seismograph network, Japan, *Lecture Notes in Earth Sciences*, **98**, 79–87, 2002a.

Obara, K., Nonvolcanic deep tremor associated with subduction in southwest Japan, *Science*, **296**, 1679–1681, 2002b.

Obara, K., Time sequence of deep low-frequency tremors in the southwest Japan subduction zone: Triggering phenomena and periodic activity, *J. Geography*, **112**, 837–849, 2003 (in Japanese with English abstract).

Obara, K., H. Hirose, F. Yamamizu, and K. Kasahara, Episodic slow slip events accompanied by non-volcanic tremors in southwest Japan subduction zone, *Geophys. Res. Lett.*, **31**(23), L23602, doi:10.1029/2004GL020848, 2004.

Okada, Y., Internal deformation due to shear and tensile faults in a half-space, *Bull. Seism. Soc. Am.*, **82**, 1018–1040, 1992.

Okada, Y., K. Kasahara, S. Hori, K. Obara, S. Sekiguchi, H. Fujiwara, and A. Yamamoto, Recent progress of seismic observation networks in Japan—Hi-net, F-net, K-NET, and KiK-net, *Earth Planets Space*, **56**, xv–xxviii, 2004.

Ozawa, S., M. Murakami, M. Kaidzu, T. Tada, T. Sagiya, Y. Hatanaka, H. Yarai, and T. Nishimura, Detection and monitoring of ongoing aseismic slip in the Tokai region, central Japan, *Science*, **298**, 1009–1012, 2002.

Ozawa, S., S. Miyazaki, Y. Hatanaka, T. Imakiire, M. Kaidzu, and M. Murakami, Characteristic silent earthquakes in the eastern part of the Boso peninsula, Central Japan, *Geophys. Res. Lett.*, **30**(6), doi:10.1029/2002GL016665, 2003.

Ozawa, S., Y. Hatanaka, M. Kaidzu, M. Murakami, T. Imakiire, and Y. Ishigaki, Aseismic slip and low-frequency earthquakes in the Bungo channel, southwestern Japan, *Geophys. Res. Lett.*, **31**(7), doi:10.1029/2003GL019381, 2004.

Rogers, G. and H. Dragert, Episodic tremor and slip on the Cascadia subduction zone: The chatter of silent slip, *Science*, **300**, 1942–1943, 2003.

Sato, H., H. Takahashi, E. Yamamoto, N. Fukuo, M. Uehara, and Y. Terasawa, Development of the crustal tilt observation method using borehole-type tiltmeters, *Zisin, 2nd ser., J. Seism. Soc. Jpn*, **33**, 343–368, 1980 (in Japanese with English abstract).

Schwartz, D. P. and K. J. Coppersmith, Fault behavior and characteristic earthquakes: Examples from the Wasatch and San Andreas fault zones, *J. Geophys. Res.*, **89**(B7), 5681–5698, 1984.

Shiomi, K., K. Obara, S. Aoi, and K. Kasahara, Estimation on the azimuth of the Hi-net and KiK-net borehole seismometers, *Zisin, 2nd ser., J. Seism. Soc. Jpn*, **56**, 99–110, 2003 (in Japanese).

Tamura, Y., T. Sato, M. Ooe, and M. Ishiguro, A procedure for tidal analysis with a Bayesian information criterion, *Geophys. J. Int.*, **104**, 507–516, 1991.

Yamanaka, Y. and M. Kikuchi, Asperity map along the subduction zone in northeastern Japan inferred from regional seismic data, *J. Geophys. Res.*, **109**, B07307, doi:10.1029/2003JB002683, 2004.

H. Hirose (e-mail: hirose@bosai.go.jp) and K. Obara